

Numerical simulation of full load surge in Francis turbines based on three-dimensional cavitating flow model

D. Chirkov¹, L. Panov¹, S. Cherny¹, I. Pylev²

¹Institute of Computational Technologies SB RAS, Novosibirsk, Russia

²OJSC "Power Machines" LMZ, St-Petersburg, Russia

chirkov@ict.nsc.ru

Abstract. The two-phase 1D-3D model of full load surge, presented previously by the authors, is applied to simulation of self-excited oscillations in prototype power station. The model consists in 1D hydro-acoustic equations for the penstock domain, and 3D two-phase unsteady RANS equations for turbine domain, including the cavitating flow in the draft tube. Both systems of equations are linked together by pressure and discharge at the penstock-turbine interface and solved simultaneously. To demonstrate the work of the model over-load pressure pulsations are simulated for high head prototype power plant. The influence of numerical parameters is investigated. It was shown that the choice of cavitation model has a strong effect on the amplitude of pulsations. The structure of the vapor cavity is investigated. The computed frequency is compared to the results of 1D model and with experimental data. Amplitudes and frequencies of the pulsations agree well with experiment, showing the potential of the method to predict full-load surge.

1. Introduction

Operation of Francis turbines in full load and overload regimes often exhibit synchronous pressure pulsations that propagate along the whole water conduit of the power plant [1,2,3]. This effect significantly restricts operation of Francis turbines at high discharge, limiting the maximum power output. The reason of these pulsations is hydrodynamic instability of swirling cavitating flow in the draft tube cone in full load operating conditions. Water system of the power plant gives positive feedback to small perturbations of vortex rope cavity volume, resulting in periodic pulsations of cavity volume, pressure, discharge and power output. This physical phenomenon, observed also in reduced scale model tests [4], yet not adequately mathematically described and simulated in CFD [5].

The state-of-the-art approach for theoretical investigation of this dynamic process is based on one-dimensional hydro-acoustic models [2-4, 6-10]. All elements of the hydraulic power plant, including the turbine, are substituted by their one-dimensional representations. The effect of cavitating vortex rope is modeled by two lumped parameters, the cavitation compliance $C = -\partial V_c / \partial H$ and mass flow gain factor (MFGF) $\chi = -\partial V_c / \partial Q$. These parameters are usually identified from experimental data [4,6] or from steady state CFD computations [4,8,10]. Explaining the phenomenon of high load pressure fluctuations, the 1D hydro-acoustic models are still far from accurate predictions of frequency and amplitude of the pulsations in prototype conditions [2,11]. One of the major reasons is uncertainty in definition of some input parameters. This is addressed to both cavitation compliance and mass flow gain factor, see discussions in [3, 5, 12], and to wave speed in the draft tube. Known uncertainty in



values of these parameters leads to intolerable discrepancy in the predictions. Then time-domain simulation of “limit cycle” oscillations, needed to evaluate the amplitude of the pulsations, is problematic. This is because time-domain simulation in frames of 1D model requires input parameters C and χ to be functions of discharge and head, introducing nonlinearity in the system. However, identification of these dependencies requires series of CFD computations [6, 10]. That is why investigation of full load pulsations is usually limited to stability and frequency analysis. One more problem with C and χ , identified from test rig measurements, consists in the need for adequate transposition of them from scale model to prototype [3], which should take into account the difference in Froude numbers.

The first step towards CFD simulation of the full load instability was done in [5], where transient cavitating flow in axially symmetric draft tube was simulated by means of two-phase CFD. Chen et. al. in [12] performed 3D two-phase simulation of the pulsating cavity in simplified conical diffuser. The authors of [5] and [12] reported low accuracy in mass conservation in the computations. This can point to non-conservativity or excessive diffusivity of the numerical scheme used in ANSYS CFX for two-phase computations.

In [13] the present authors suggested a more general hybrid 1D-3D model and numerical method for simulation of pressure and discharge surge in the whole hydraulic system of a power plant. The model consists of 1D hydro-acoustic equations for the penstock and 3D Reynolds-Averaged Navier-Stokes equations for the two-phase flow in turbine and draft tube. Both systems of equations are linked together by pressure and discharge at the penstock-turbine interface and solved simultaneously. It was shown in [13] that the model was able to capture self-excited oscillations of cavitating vortex rope observed in full-load operating points. However, test computations in [13] were held for a scale model turbine with artificial parameters, not allowing to compare the results with experiment. In [14] the model was applied to simulate over-load pressure pulsations in prototype power plant. It is shown in [13,14] that the computed frequency of the pulsations qualitatively agrees with the experimental trends. In particular, it was shown that reducing the Thoma number, enlarging the length of the penstock and increasing discharge, act to reduce the pulsation frequency.

In the present paper the 1D-3D model from [13] is further investigated in application to over-load instability on high head prototype power plant. First, the influences of numerical parameters, such as mesh size, time step, as well as the influence of cavitation model are analyzed. In particular, it is shown that cavitation model has a strong impact on the amplitude of pulsations. The 3D structure of the cavity volume is investigated. Also a comparison with fully 1D model is carried out in terms of frequency of the pulsations. Then the method is applied to the comparison of pressure pulsations for two variants of the runner. The computed results are compared with available experimental data for one of the runners.

2. 1D model

One of the goals of the present paper was to compare the predictions of 1D-3D model with fully 1D model. Thus for completeness, let us briefly describe the fully 1D model of the power plant [6, 7]. For simplicity, assume the power plant consisting of the penstock, Francis turbine, and draft tube, see Figure 1.

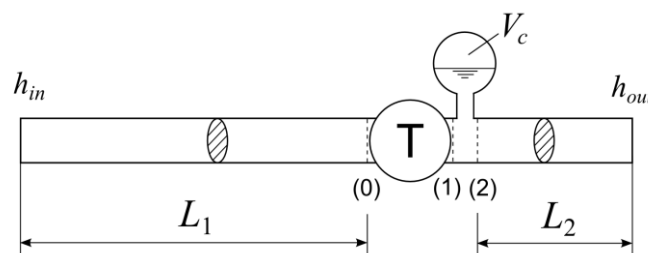


Figure 1. Scheme of 1D hydro-acoustic model.

Hydro-acoustic equations for the penstock pipe of length L_1 are:

$$\begin{cases} \frac{\partial h}{\partial t} + \frac{a_1^2}{gA_1} \frac{\partial Q}{\partial x} = 0 \\ \frac{\partial Q}{\partial t} + gA_1 \frac{\partial h}{\partial x} = 0 \end{cases} \quad (1)$$

HA equations for the draft tube of length L_2 :

$$\begin{cases} \frac{\partial h}{\partial t} + \frac{a_2^2}{gA_2} \frac{\partial Q}{\partial x} = 0 \\ \frac{\partial Q}{\partial t} + gA_2 \frac{\partial h}{\partial x} = 0 \end{cases} \quad (2)$$

Here $h = p/(\rho_L g) - z$ is the piezometric head (note, that Oz axis is directed downwards); Q is the discharge; a_1, a_2 are the wave speeds in penstock and draft tube, respectively; A_1, A_2 are the cross sections of penstock and draft tube, respectively; t is time and x is the coordinate along the length of the flow passage. Friction loss and viscoelastic damping, caused by energy dissipation during the pipe wall deflection, are both neglected.

In order to link the above hydro-acoustic equations of penstock and draft tube, one has to add equations, responsible for turbine (without the draft tube) and for vapor volume in the upper part of the draft tube cone. The turbine is represented by its inertia $L_t = \bar{I}_t / (g\bar{A}_t)$ and pressure sink term $H_t = H_t(Q_{(0)})$. The latter is taken from steady state discharge-head characteristic of the turbine for the fixed guide vane opening. Compressibility of flow in turbine is neglected. Therefore the flowing equations are used to link the flow parameters h and Q in penstock outlet section (0) and runner outlet section (1), see Figure 1:

$$\begin{cases} L_t \frac{dQ_{(0)}}{dt} = h_{(0)} - h_{(1)} - H_t \\ Q_{(0)} = Q_{(1)} \end{cases} \quad (3)$$

Vapor cavity in the draft tube cone is represented by its cavitation compliance C and mass flow gain factor χ [6]

$$\begin{cases} C \frac{dh_{(2)}}{dt} + \chi \frac{dQ_{(*)}}{dt} = Q_{(1)} - Q_{(2)} \\ h_{(1)} = h_{(2)} \end{cases} \quad (4)$$

Here for definiteness the MFGF is attributed to downstream discharge, as in [6, 8, 12], so $Q_{(*)} = Q_{(2)}$ in (4). It should be noted that thermodynamic damping, modeling the energy dissipation due to phase exchange between liquid and gas, introduced recently in [3,10], is neglected in the present model.

Boundary conditions $h = \text{const} = h_{in}$ in penstock inlet and $h = \text{const} = h_{out}$ in draft tube outlet close the governing equations (1)-(4) of 1D model.

The key (and most uncertain) parameters of the model are C , χ and a_2 . The solution of system (1)-(4) can be found numerically. For this, spatial derivatives in hyperbolic equations (1) and (2) are discretized using central-difference approximation on a staggered grid [7]. This results in a system of ordinary differential equations

$$\mathbf{A} \frac{d\mathbf{Y}}{dt} + \mathbf{B}\mathbf{Y} + \mathbf{C} = 0, \quad (5)$$

that can be solved in time-domain using Runge-Kutta method. In the present paper only the stability analysis of system (5) is performed, requiring just the evaluation of complex eigenvalues λ_k of matrix $-\mathbf{A}^{-1}\mathbf{B}$ [7, 10].

3. Hybrid 1D-3D two-phase model

In the hybrid model [13] wave propagation in penstock is simulated using hydro-acoustic equations (1), as in 1D model, while the flow-field in turbine and draft tube is governed by unsteady 3D 2-phase RANS equations, Figure 2. The solution in both parts is found simultaneously.

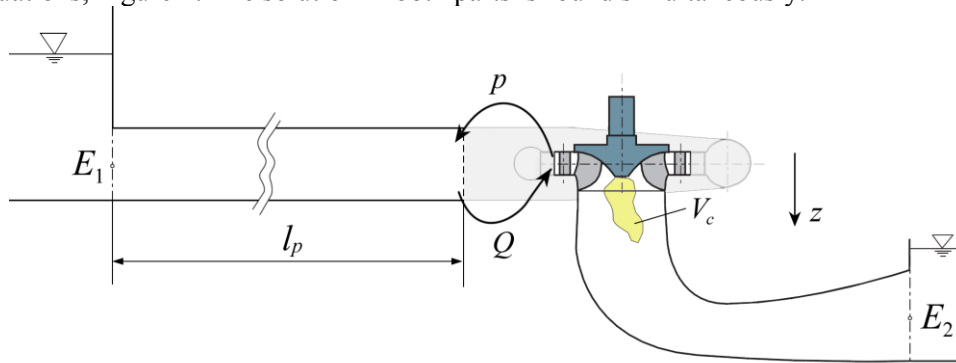


Figure 2. Computational domain for 1D-3D model.

Cavitating flow inside the turbine and draft tube is described as isothermal compressible “liquid–vapor” mixture, where distribution of liquid volume fraction α_L is described by transport equation with source terms, responsible for evaporation and condensation:

$$\frac{\partial \rho}{\partial t} + \text{div}(\rho \mathbf{v}) = 0, \quad (6)$$

$$\frac{\partial \rho \mathbf{v}}{\partial t} + \text{div}(\rho \mathbf{v} \otimes \mathbf{v}) + \nabla \hat{p} = \text{div}(\boldsymbol{\tau}) + \rho \mathbf{f}, \quad (7)$$

$$\frac{\partial \alpha_L}{\partial t} + \text{div}(\alpha_L \mathbf{v}) = \frac{1}{\rho_L} (m^+ + m^-). \quad (8)$$

Here $\rho = \alpha_L \rho_L + (1 - \alpha_L) \rho_V$ is the mixture density, \mathbf{v} is the velocity vector, $\hat{p} = p + \frac{2}{3} \rho k$, p is the static pressure; k is the turbulence kinetic energy. Absolute reference frame is used for static elements, while rotating reference frame is used for the runner, rotating with angular velocity ω around the Oz axis. Thus for runner sub-domain $\mathbf{f} = (x_1 \omega^2 + 2u_2 \omega, x_2 \omega^2 - 2u_1 \omega, g)$. Kim-Chen k - ε turbulence model with log-law wall function near the solid walls is used to close the mean flow equations (6)-(8).

Two cavitation models are used in the present paper for evaluation of condensation (m^+) and evaporation (m^-) terms in (8). The first is Singhal et. al. model [15],

$$m^+ = \frac{C_{prod} \max[p - p_V, 0] 1 - \alpha_L}{t_\infty \rho_L U_\infty^2 / 2}, \quad m^- = \frac{C_{dest} \min[0, p - p_V] \rho_L^2 \alpha_L}{\rho_V t_\infty \rho_L U_\infty^2 / 2}, \quad (9)$$

where $C_{prod} = 80$, $C_{dest} = 1$. The second is Zwart–Gerber–Belamri (ZGB) model [16]:

$$m^+ = C_{prod} (1 - \alpha_L) \rho_V \sqrt{\frac{2 \max[0, p - p_V]}{3 \rho_L}}, \quad m^- = -C_{dest} \alpha_L \rho_V \sqrt{\frac{2 \max[0, p_V - p]}{3 \rho_L}}, \quad (10)$$

where $C_{prod} = 3 \cdot 10^4$, $C_{dest} = 7.5 \cdot 10^4$.

4. Numerical method and boundary conditions

The above 1D-3D model is implemented within the in-house developed CADRUN solver (Computer Aided Design of RUNner). Two-phase fluid flow equations (6)-(8) are solved numerically using artificial compressibility method. Dual time stepping is used for unsteady calculations. In pseudotime equations are marched using implicit finite volume scheme. Third order accurate MUSCL scheme is used for discretisation of convective terms, while 2nd order central difference scheme is used for viscous terms. Second order backward scheme is applied for physical time derivatives. Linearized system of discrete equations is solved using LU-SGS iterations. All equations (6)-(8) are solved in terms of (p, v, α_L) in a coupled manner. For more details reader is referred to [17].

Periodic stage approach is used for the turbine flow analysis, requiring computations only in one wicket gate (WG) channel, one runner channel, and the whole draft tube (DT). Mixing plane boundary condition is applied on “WG – runner” and “runner – DT” interfaces with circumferential averaging of all flow variables $(p, u, v, w, \alpha_L, k, \epsilon)$. Hydro-acoustic equations (1) are solved using 1st order implicit finite difference scheme. Equations (1) and (6)-(8) are iterated in pseudotime simultaneously until convergence. During the iterative solution of hydro-acoustic and two-phase equations flow parameters are exchanged through artificial “penstock – wicket gate” interface. Implementation of this condition is described in detail in [13].

Total specific energy E_2 at draft tube outlet is obtained from a given Thoma number σ and net head H according to IEC 60193 standard

$$E_2 = \sigma H + \frac{p_v}{\rho_L g} - z_r, \quad (11)$$

where z_r is the reference level, evaluated from the upper ring of wicket gate ($z = 0$). This condition is accompanied by the hydrostatic equation $\partial p / \partial z = \rho_L g$ in the draft tube outlet section. Total specific energy is fixed at the inlet of the penstock

$$E_1 \equiv \left(h + \frac{Q^2}{2gA_1^2} \right) = E_2 + H = \text{const}. \quad (12)$$

It should be noted, that discharge is not fixed anywhere, and is obtained as a part of the solution.

5. Numerical results

The suggested hybrid model is applied to the analysis of over-load surge in prototype power plant with specific speed $n_s=200$ and maximum head 220 m. Two runners were considered for this power plant: old runner (R1), designed in the early 1980's and new runner (R2), designed recently. Considered is the overload operating point with 15% increased power ($Q = 1.17Q_{opt}$), where strong pressure pulsations had been observed for the old runner. Preliminary computations showed that the two-phase flow-fields in the draft tube are different for the two runners, Figure 3. For R2 the flow is almost axially symmetric in the upper part of the draft tube, while for the old runner R1 the cavity is not symmetric, tending to a helical shape as in part load conditions. This is due to the deficit of axial velocity near the hub behind the runner R1. Therefore mixing plane condition at the inlet of the draft tube does not work well for the old runner. In order to exclude this error, the influence of numerical and model parameters is investigated for the new runner R2.

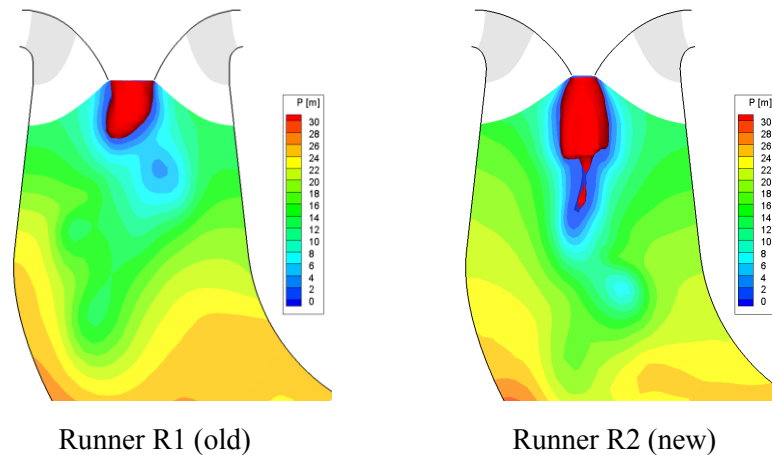


Figure 3. Contours of pressure and iso-surface $\alpha_L = 0.5$ (red) for two runners.

5.1. Sensitivity to numerical parameters for runner R2

This subsection shows the influence of mesh, time step and cavitation model on the computed overload pulsations for R2 runner. Simulations are carried out using two computational meshes: coarse (150.000 cells) and fine (400.000 cells), that differs from the coarse mesh only in the draft tube region. Fine computational mesh is shown in Figure 4. Input parameters of 4 runs are presented in Table 1.

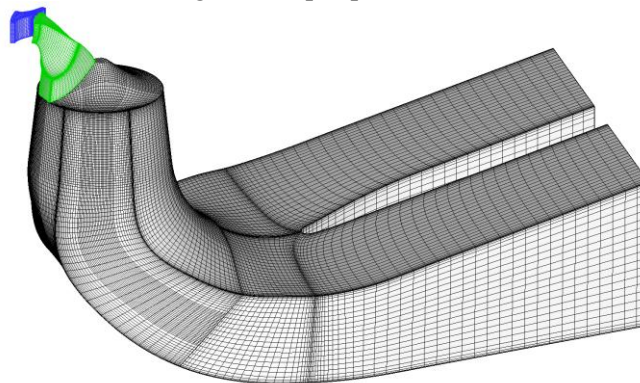


Figure 4. Fine CFD mesh for wicket gate, runner and draft tube domains.

Computational procedure is the following. First, steady state two-phase flow-field without the penstock is computed. Then the penstock is attached and unsteady two-phase computations are set up. As in [Чирков_2010] the coarse time step Δt is taken $1/24$ of runner rotation period. Taking into account that characteristic frequency of synchronous pulsations falls into interval $0.3-0.5 f_n$, one period of pulsations is covered by 50-70 time steps.

In all unsteady computations we get almost periodic pulsations of pressure, discharge and cavity volume, Figures 5,6. Pressure pulsations in WG and on the draft tube wall are in phase. Peak-to-peak amplitude of pulsations, obtained using ZGB model is about 2% of the net head in the DT, and about 4% in WG. At that the amplitude of discharge pulsations in WG is approximately 0.6%.

It can be seen in Figure 5, that within ZGB model spatial mesh and time step refinement have a little influence on frequency, but affect the amplitude of the pulsations, see also Table 1. However this influence is not crucial.

The major impact on amplitude of the pulsations gave the choice of cavitation model. Switch from ZGB to Singhal model (run #4) two times increased the amplitude of surge. Apparently, this effect is caused by the fact, that Singhal model (9) has a more intensive evaporation term m^- , in comparison to corresponding term ZGB model (10). It should be noted that strong difference in the

computed results, obtained with these cavitation models appeared only in unsteady calculations. Our previous steady state computations of cavitation characteristics of Francis turbines showed almost identical predictions, obtained by ZGB and Singhal models [17]. Therefore future choice and calibration of cavitation model should be done on the basis of unsteady test cases with detailed experimental data.

In order to check the consistency of 2-phase solution it is suggested in [Дорфлер_2010] to check the accuracy of mass conservation in the computed flow field. Following [Дорфлер_2010, Chen_2010] we have calculated both sides of the equation:

$$\frac{dV_c}{dt} = Q_{DT1} - Q_{DT2}, \quad \text{where} \quad V_c = \int_V (1 - \alpha_L) dV, \quad Q = \frac{1}{\rho_L} \int_S \rho(\mathbf{v} \cdot d\mathbf{S}). \quad (13)$$

Here Q_{DT1} , Q_{DT2} are the volumetric discharges in draft tube entrance and elbow exit, respectively. Figure 7 shows fulfillment of equation (13) for Singhal model (run #4). It can be seen that mass conservation is fulfilled with tolerable accuracy, as in the former computations of scale model turbine [13]. This result may be due to the coupled solution of equations for pressure, momentum and α_L in the present numerical method.

Figure 8 demonstrates the evolution of two-phase flow-field in the draft tube cone in different time moments within one period of the pulsations, obtained with the fine mesh (run #3). It can be seen that axially symmetric cavity in the upper part of the draft tube breaks up downstream, with the formation of a rotating screw-like vortex rope. The frequency of its rotation is approximately 5 times higher than the frequency of cavity volume pulsations. However this vortex rope is of small intensity, so its rotation gives insignificant contribution to pressure pulsations on DT wall.

It was interesting to compare the computed pulsation frequency with the unstable frequencies found in frames of 1D model. For this reason eigenvalues $\lambda_k = \delta_k + i\omega_k$ of system of ordinary differential equations (5) have been calculated for C varying from 0.01 m² to 1.0 m², and χ varying from -0.1 s to 0 s. Draft tube wave speed a_2 was taken in the range 100 – 1200 m/s. Real part δ_k is the damping coefficient, while imaginary part ω_k is the oscillation frequency of the eigen mode. Unstable modes are those with $\delta_k > 0$. It was found that first unstable frequency just slightly depends on the value of χ . Figure 9 shows the dependency of first unstable frequency on C for different values of wave speed a_2 . It can be seen that at $a_2=1200$ m/c (which is closest to the conditions of 1D-3D hybrid model, where $a_2 = \infty$) the CFD frequency $f = 0.35f_n$ is reached only at $C = 0.45$ m².

Then the value of cavitation compliance and mass flow gain factor were identified from series of steady state two-phase CFD computations, with different draft tube outlet energy and discharge. It was found that $C = 0.135$, $\chi = -0.05$. With that value of cavitation compliance, 1D model gives the frequency $f = 0.59f_n$, that is higher than $f = 0.35f_n$, obtained in unsteady CFD computations.

Table 1. Comparison of frequency and amplitude of pressure pulsations.

# of run	Cavitation Model	Mesh	Time step, $\Delta t/T_R$	Frequency of pulsations f/f_n	Pressure pulsation amplitude before GV $(2A/H) \cdot 100\%$	Pressure pulsation amplitude in DT cone $(2A/H) \cdot 100\%$
1	ZGB	Coarse	1/24	0.356	4.0	2.0
2	ZGB	Fine	1/24	0.351	3.6	1.5
3	ZGB	Fine	1/48	0.348	3.9	1.8
4	Singhal	Coarse	1/24	0.330	8.2	5.3

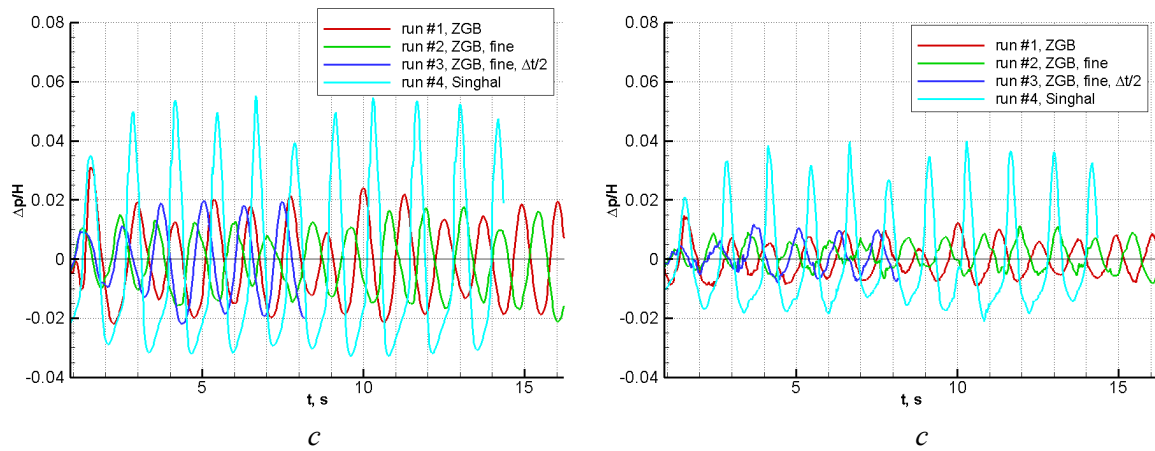


Figure 5. Pressure pulsations before the guide vanes (left) and on draft tube wall (right).

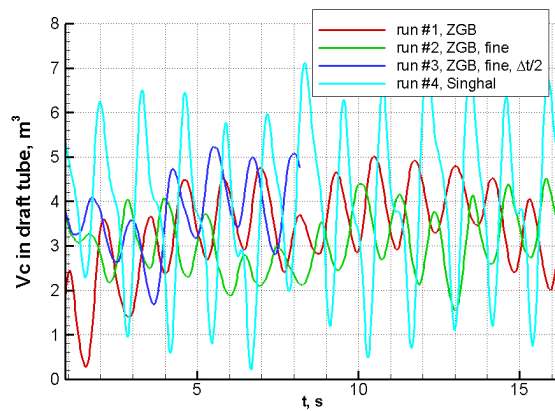


Figure 6. Pulsations of cavity volume V_c .

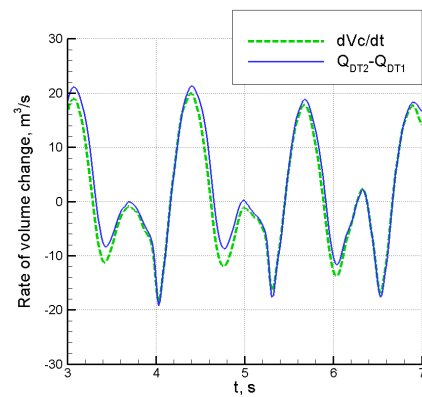


Figure 7. Mass conservation check for Singhal model.

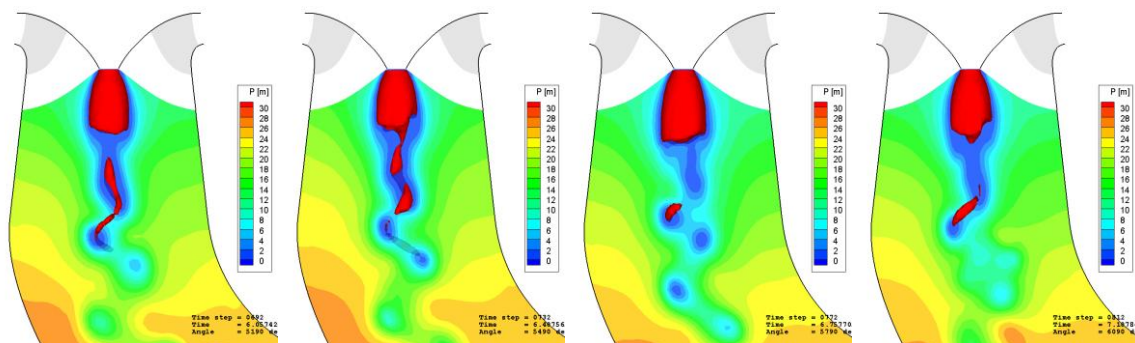


Figure 8. Runner R2. Flow field in draft tube cone over 1 period of pulsations. Contours of pressure and iso-surface $\alpha_L = 0.5$ (red).

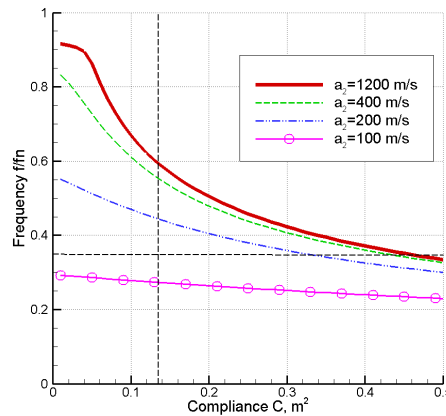


Figure 9. First unstable frequency in 1D model for runner R2.

5.2. Comparison of two runners

This section presents the results of comparison of pressure pulsations for runners R1 and R2 in the same overload operating point, and comparison with experiment for runner R1. ZGB cavitation model, coarse mesh and time step $\Delta t = T_R / 24$ were used for the simulations. Figure 10 shows the comparison of pressure pulsations in WG and DT, as well as oscillations of cavity volume V_c . Pulsations in old runner R1 are less periodic, due to more complex structure of flow field in the upper part of the draft tube cone. The average amplitude of draft tube pulsations is approximately the same for old and new runners, while amplitude of pulsations upstream in the wicket gate is almost twice less for the new runner. At that the average cavity volume for R2 runner is 3 times larger, than for R1.

5.3. Comparison with experiment

Table 2 and Figure 11 show the comparison of frequency and peak-to-peak amplitude of pressure pulsations with experimental data for the old runner. Three operating points have been computed, corresponding to relative discharge 1.13, 1.17, and 1.20. The computed frequency is 7-15% lower than in experiment. The amplitude of pressure pulsations agree with experiment for $Q/Q_{opt} = 1.13$, and slightly underestimated for higher discharge.

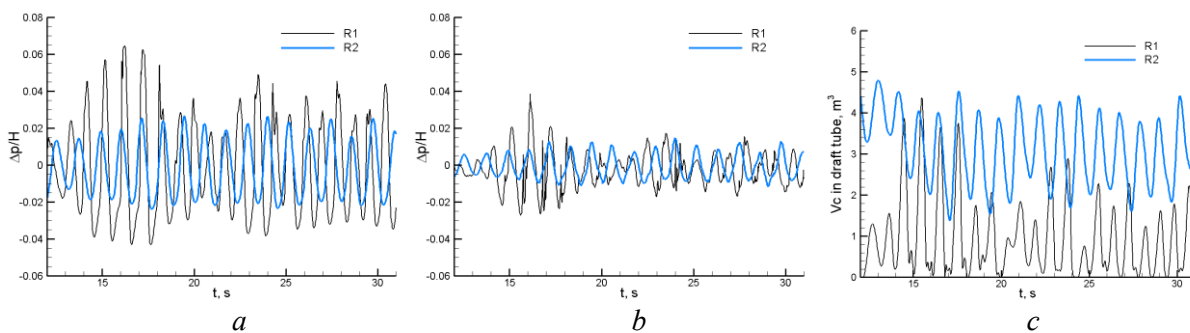
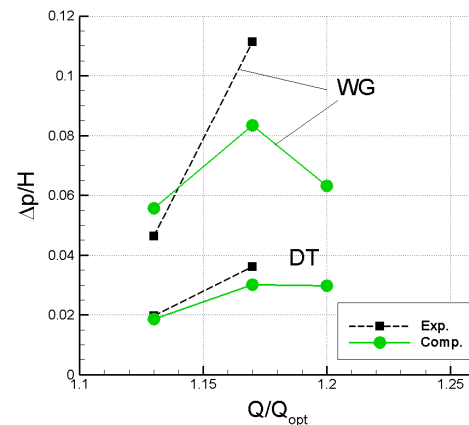


Figure 10. Pulsations of pressure in WG (a) and DT (b), and oscillation of cavity volume V_c (c) in draft tube for runners R1 and R2.

Table 2. Relative frequency of pulsations, f/f_n for runner R1

Q/Q_{opt}	1.13	1.17
Experiment	0.58	0.57
Computation	0.54	0.48-0.51

**Figure 11.** Amplitude of pressure pulsations in WG and DT for the old runner.

6. Conclusion

In the present paper the two-phase 1D-3D model of full load surge, presented previously by the authors, is applied to simulation of self-excited oscillations in prototype power station. The model consists in 1D hydro-acoustic equations for the penstock domain, and 3D two-phase unsteady RANS equations for turbine domain, including the cavitating flow in the draft tube. Theoretically the model takes into account all the factors, accounted in fully 1D models, except for the finite wave speed in the draft tube. However, the 1D-3D model is free from some of the shortcomings of one-dimensional models of full load surge. The most important, it does not require definition of cavity compliance C and mass flow gain factor χ . Iterative linking of penstock and turbine flow parameters during the simultaneous solution of both systems of equations ensures the stability of conjugated computation. Thus the presented model and numerical method offer wide capabilities for the investigation of full load pulsations.

As an example, over-load pressure pulsations are investigated for high head prototype power plant. It was shown that the choice of cavitation model has a strong effect on the amplitude of pulsations. Computations show that in prototype conditions the vapor cavity is axially symmetric only in upper part of the draft tube, and breaks up downstream with the formation of screw-like vortex with high rotating frequency. The computed frequency does not agree well with frequencies, obtained through stability analysis of fully 1D model. The reason of this discrepancy should be further investigated.

Operation of two runners in over-load operating point has been compared. It was shown that the new runner has 2 times smaller amplitude of pulsations, than the old one. Amplitudes and frequencies of the pulsations agree well with the experimental data, showing the potential of the method to predict full-load surge. From the other hand, computations show the need for the improved unsteady cavitation model, and necessary switch to computation of the whole runner, rather than one runner channel. The influence of turbulence model should also be investigated. In future the authors plan to add the third phase, namely, non-condensable air, to account for the air injection, which in some cases helps to reduce or even completely eliminate the full load pulsations.

Acknowledgments

This work was partly supported by grant № 14-01-00278 of Russian Foundation for Basic Research.

Nomenclature

a	Wave speed [m/s]	Q	Discharge [m ³ /s]
C	Cavity compliance [m ²]	A	Cross section area [m ²]
E	Specific total energy [m]	V_c	cavity volume [m ³]

G	Gravity [m/s^2]	α_L	Liquid volume fraction [-]
H	Net head [m]	χ	Mass flow gain factor [s]
h	Piezometric head ($= p / \rho_L g - z$) [m]	ρ	Mixture density [kg/m^3]
n_s	specific speed ($= 3.65 n_{11} \sqrt{Q_{11} \eta}$)	ρ_L	Water density [kg/m^3]
p_V	Vapor pressure [Pa]	ρ_V	Vapor density [kg/m^3]

References

- [1] Jacob T and Prenat J-E 1996 Francis Turbine Surge: Discussion and Data Base *IAHR Symp. on Hydraulic Machinery and Systems* (Valencia, Spain)
- [2] Koutnik J, and Pulpitel L 1996 Modeling of the Francis turbine full-load surge. *Modeling, Testing and Monitoring for Hydro Power plants* (Lausanne, Switzerland).
- [3] Dörfler P 2009 Evaluating 1d models for vortex-induced pulsation in francis turbines. *3rd Int. Meeting of the Workgroup on Cavitation and Dynamic Problems in Hydraulic Machinery and Systems* (Brno, Czech Republic) **2** pp. 315-324.
- [4] Alligne S, Maruzewski P, Dinh T, Wang B, Fedorov A, Iosfin J and Avellan F 2010 Prediction of a Francis turbine prototype full load instability from investigations on the reduced scale model *IAHR Symp. on Hydraulic Machinery and Systems* (Timisoara, Romania)
- [5] Dörfler P K, Keller M and Braun O 2010 Francis full-load surge mechanism identified by unsteady 2-phase CFD *IAHR Symp. on Hydraulic Machinery and Systems*
- [6] Koutnik J, Nicolet C, Schohl G A and Avellan F 2006 Overload surge event in a pumped storage power plant *IAHR Symp. on Hydraulic Machinery and Systems* (Yokohama, Japan).
- [7] Nicolet C 2007 Hydroacoustic modelling and numerical simulation of unsteady operation of hydroelectric systems. Ph. D. Thesis EPFL No. 3751
- [8] Flemming F, Foust J, Koutnik J and Fisher R K 2008 Overload surge investigation using CFD data *IAHR Symp. on Hydraulic Machinery and Systems* (Foz do Iguassu, Brazil)
- [9] Chen C, Nicolet C, Yonezawa K, Farhat M, Avellan F, Tsujimoto Y 2008 One-dimensional analysis of full load draft tube surge *J. of Fluids Engineering* **130**
- [10] Alligne S, Nicolet C, Ruchonnet N, Hasmatuchi V, Maruzewski P, Avellan F 2009 Numerical simulation of nonlinear self-oscillations of a full load vortex rope *3rd Int. Meeting of the Workgroup on Cavitation and Dynamic Problems in Hydraulic Machinery and Systems* (Brno, Czech Republic) **2** pp. 325-338.
- [11] Alligne S 2011 Forced and self oscillations of hydraulic systems induced by cavitation vortex rope of Francis turbines. Ph. D. Thesis, EPFL No. 5117.
- [12] Chen C, Nicolet C, Yonezawa K, Farhat M, Avellan F, Miyagawa K, Tsujimoto Y 2010 Experimental study and numerical simulation of cavity oscillation in a conical diffuser *Int. J. of Fluid Machinery and Systems* **3** No. 1, p. 91-101.
- [13] Chirkov D, Avdyushenko A, Panov L, Bannikov D, Cherny S, Skorospelov V, Pylev I 2012 CFD simulation of pressure and discharge surge in Francis turbine at off-design conditions *IAHR Symp. on Hydraulic Machinery and Systems* (Beijing, China)
- [14] Panov L V, Chirkov D V, Cherny S G, Pylev I M 2014 Numerical simulation of pulsation processes in hydraulic turbine based on 3D model of cavitating flow *Thermophysics and Aeromechanics* **21** No. 1.
- [15] Singhal A K, Vaidya N and Leonard A D 1997 Multi-dimensional simulation of cavitating flows using a PDF model for phase change. ASME Paper FEDSM97-3272
- [16] Zwart P J, Gerber A G, Belamri T A 2004 Two-phase flow model for predicting cavitation dynamics. ICMF 2004 International Conference on Multiphase Flow. Paper No. 152 (Yokohama, Japan).
- [17] Panov L V, Chirkov D V, Cherny S G, Pylev I M and Sotnikov A A 2012 Numerical modeling of steady-state cavitation flow of viscous fluid in Francis hydroturbine *Thermophysics and Aeromechanics* **19** No. 3 p. 415-427